ECS Transactions, 29 (1) 23-31 (2010)
10.1149/1.3532300 ©The Electrochemical Society

Novel SVET Approach and its Application for Rapid Pitting Corrosion Studies of Chromatized Aerospatiale Aluminum Alloy

R. Ramos, R. K. Zlatev, M. S. Stoytcheva, B. Valdez, S. Kiyota

Instituto de Ingeniería, Universidad Autónoma de Baja California, Mexicali 21280, México

The controversial statements reported till now about the local conductivity of the solution at its interface with the corroded specimen affecting the SVET results were verified by the simultaneous application of a combination of two measuring techniques: SVET and conductometry. Bare and chromatized AA 6061-T6 aerospatial aluminum alloy samples in 5% NaCl solutions were employed in the experiments. It was confirmed that the local conductivity variations are negligible above the chromatized specimens obviously because of the pit sealing while about 4% changes were observed 5 minutes after the immersion of the bare samples. An approach for fast automatic detection of pit sites on the entire specimen surface, based on high resolution digital optical scanning coupled with image recognition software was developed and applied in the SVET/Conductivity experiments.

Introduction

The Scanning Vibrating Electrode Technique (SVET), first developed for biological applications (1), was further improved by Isaacs (2, 3) and applied for pitting, inter-granular or galvanic corrosion studies. SVET known also as Scanning Vibrating Probe (SVP) or Current Density Probe (CDP) allows the determination of the current distribution above the local anodic and cathodic electrochemical reactions that happen on the freely corroding metal surface. The ionic current flowing through the solution between the anodic and the cathodic zones of the corroded surface causes occurring of a potential gradient depending on the local solution conductivity and decays with the distance from the corroded surface. A basic study on these phenomena has been reported by Wagner (4). Being a further improvement of the Scanning Reference Electrode Technique developed earlier (SRET) (5, 6), SVET provides higher sensitivity due to its higher signal to noise ratio (S/N): while the potential gradients measured by SRET are about 200 μV, gradients as low as 5 μV are measurable by SVET (7-10). These values are limited by the noise level.

The mechanical vibration of the SVET sensing probe converts the DC potential gradient in AC signal with the frequency of the probe vibration and amplitude proportional to the ion current density above the corroded specimen. By the application of a lock-in-amplifier (LIA) able to recover AC signals with known frequency from very noisy environments (-60 dB), the appearing AC signal is separated and measured.

Local measuring techniques combinations allow more complete characterization of the localized corrosion processes (11). Ogle et al. (12) applied local pH and current

density measurements to galvanized steel cut edge corrosion. Park et al. (13) reported a combination of pH measurement and polarization curves registration at local corrosion sites containing MnS inclusions. Vuillemin et al. (14) reported a combination of SVET, AFM and SAM (Scanning Auger Microscopy) applied to pitting corrosion of a MnS inclusion on 316L stainless steel, employing aggressive solution injection (NaCl, H_2SO_4 or HCl).

As established by Oltra et al. (11), significant changes in solution chemistry may occur very close to the corroded surface, so that the conductivity may be unknown and some of the currents can be controlled by diffusion as well. For example dynamic local change in surface composition due to precipitation of dissolved species coming from inclusion dissolution has been reported by Vuillemin et al. (14). Thus, the effect of the ohmic drop which stabilizes the localized corrosion processes becomes part of the electrochemical polarization of the system in terms of electrochemical kinetics (11).

On the other hand Deshpande (15) stated that the solution conductivity increase is marginal (less than 0.4%) confirming that there was no difference in the conductivity values, closer to the galvanic couple and in the bulk solution.

The mentioned controversial statements determine the need of real time local conductivity monitoring at the nearest surface environments together with the SVET measurements and this is the objective of the present work. An approach allowing fast pits detecting was applied, based on high resolution specimen digital scanning coupled with image recognition software application yielding probable pits coordinates database used further for automatic SVET scanning of the probable pit sites only jumping over the unaffected areas.

Experimental

Specimens Preparation and Testing Electrolyte Composition and Concentration

The approach subject of the present work was tested using 1 by 1 cm bare and chromatized AA 6061 T3 airspace aluminum alloy specimens. Salt spray testing procedure according to the ASTM B117 standard requirements was applied to provoke pits appearing. The alodining process was applying for the chromatizing yielding: $Cr(OH)_2HCrO_4$ and $Cr_2O_3.1.2H_20$ (48 to 80 %); Al_2O_3, AlF_3, AlOF, AlOOH (15 to 30 %) coatings composition. Although the detailed mechanisms by which Cr^{6+} decreases the corrosion rate of Al alloys are still unclear (16) Cr^{6+} inhibits the cathodic reactions (primarily oxygen reduction) and the active sites in the alloy (17).

Non-buffered 5% (0.86mol dm^{-3}) NaCl solutions with a conductivity of 7.01 Sm^{-1} at 20°C was used in all the experiments. This relatively high salt concentration was chosen to obtain a measurable signal employing small size conductometric electrodes (vibrating probe tips).

SVET / Conductometric Equipment

Home made equipment was applied for the pitting corrosion studies employing two vibrating probes setup allowing SVET and conductivity measurements. One of the probe

tips was used for SVET measurements and both for the conductometric ones. For every step of the surface scan the SVET signal was registered and a sine wave voltage was applied between the probes and the corresponding AC current was registered. A NI USB 6009 Data Acquisition System coupled with NI Lab View software were used for SVET and conductivity measurements, as well as for the application of the conductometric sine wave voltage with amplitude of 100 mV p-p and frequency of 60 Hz, synchronized with the power line. The same frequency was applied for the SVET probe vibration and as reference frequency of the lock-in amplifier.

A PC controlled linear stage mechanisms allowing fast positioning of the vibrating probe were employed for X and Y coordinate specimen scanning. A voltage driven lens focusing mechanism taken from a CD drive was employed for Z direction positioning of the probes (within 1.5 mm) and its vibration with amplitude of 10 μm at 50 μm distance from the specimen. All the movements of the vibrating probe were computer controlled by proper NI Lab View software application.

Digital Optical Scanning and Image Recognition Software

A commercial Epson Perfection V750-M Pro scanner with optical resolution of 9600/6400 dpi allowing 2.65 by 3.97 μm areas distinction on the sample surface was applied for the digital image acquisition of the corroded sample. The output JPEG file was further processed by a home made image recognition software yielding: a) probable pits recognition; b) real pits distinction from pits looking stains; c) coordinates of the probable pits virtual centers and equivalent diameter determination vs. the sample zero and d) creation of database of pits areas to be scanned by SVET/conductometry equipment.

While some false pits recognition as real (probable) leads to SVET measuring time increase only, the real pits not recognized by the software decrease the reliability of the proposed approach. That is why the recognition threshold of the software was chosen low and the pits having 50% or more calculated probability were included in the data base to be scanned by the SVET equipment.

Results and Discussion

SVET signal calibration

The equation (1) allows the conversion of the measured potential gradient in current density (12):

$$j = \sigma\,(\Delta E/A) \qquad [1]$$

where:
j is the current density in A m^{-2};
σ is the conductivity of the electrolyte solution assumed to be a constant.
ΔE is the potential difference across the vibration amplitude in V;
A is the vibration amplitude.

Since σ and A are constants, the equation [1] can be presented simpler as: $j = K\,\Delta E$. Thus, the aim of the SVET calibration is the determination of the coefficient K. For this purpose an acrylic cell with two Pt disc electrodes 25 μm in diameter placed on its bottom was employed. Known constant currents (j) in the range from 0.2 to 10 μA were imposed between the two Pt electrodes by the application of a galvanostat and the surface above the Pt micro-disc anode was scanned by the SVET probe vibrating with 10 μm amplitude at a constant height of 50 μm. The maximal potential gradient ΔE measured at the center of the Pt anode was plotted against the imposed current values and the coefficient K determined as the slope of the curve was found to be 7.82×10^5 A V^{-1} m^{-2}.

Conductometer calibration

NaCl water solutions with known concentrations in the range from 5 to 10 Sm^{-1} were employed for conductometer calibration. The measured AC current flowing between the two probe tips (caused by the imposed AC voltage with 100 mV p-p amplitude) was plotted against the solution conductivity. The calibration curve has the following characteristics: b[0] = 1.06 and b[1] = 0.07

Current density/conductivity mapping

Control samples experiments. They involve bare Al 6061-T3 specimens in 5% NaCl solution were carried out as a reference. The bare metals exhibited one or more dynamic zones of anodic activity, reflecting sites of localized corrosion. The pits appeared almost immediately, with the observation of significant currents flowing during the first SVET scan and then decaying rapidly because of the passivation on a time scale of tens of minutes.

Family of SVET profiles registered by multiple X scan of same pit area (Y = 0) every 5 minutes during 20 minutes are shown in Fig. 1 (left). The anodic current decreases with the time because of the passivation (curves **a** to **d**), while the cathodic sites are affected by corrosion products precipitation provoking the same effect.

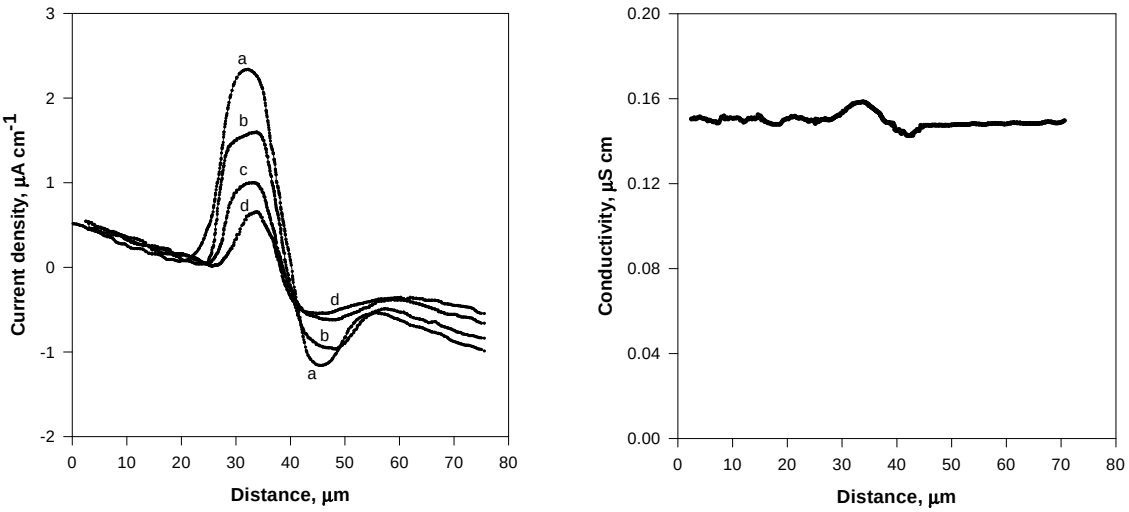

Figure 1. Current density (left) and local conductivity (right) profiles above a pit site

The conductivity profile corresponding to the SVET curve **a** and registered simultaneously 5 minutes after the specimen immersion is shown in Fig.1 (right). A 4.8% increase observed above the anodic zone due to the metal dissolution while the cathodic current decrease with 4.0% probably due to the corrosion products precipitation caused by the increased pH according to the cathode reaction:

$$O_2 + 2H_2O + 4e^- = 4OH^- \qquad [2]$$

The obtained values for the local conductivity are much higher than those reported by Deshpande (15) but not indicating "significant changes in solution chemistry" as stated by Oltra et al. (11). The registered conductivity decreases with the time due to the corrosion products precipitation and becomes rather undistinguishable from the noise 7 minutes after the immersion.

The time dependent anodic current decrease was studied by potentiodynamic Tafel plots as well. Two curves were registered 5 minutes (curve **a** in Fig. 2) and 40 minutes (curve **b** in Fig. 2) after immersion of the specimen in the test solution. The entire specimen surface was covered by polymer resin except the studied pit. As shown in Fig. 2, the anodic current decays about 10 times while the pitting potential remains almost the same during the time of immersion.

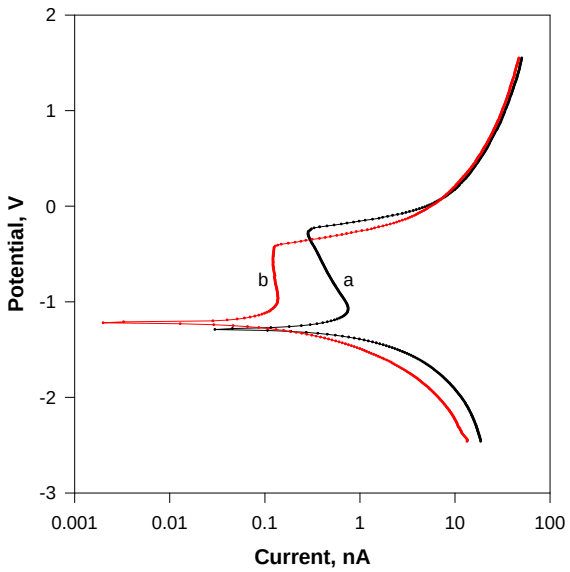

Figure 2. Tafel plots of bare airspace 6061-T6 aluminum alloy: curve a, 5 minutes of immersion; curve b, 20 minutes of immersion in 5% NaCl test solution

Chromatized samples experiments. They were carried out using specimens chromatized by alodining process including 60 s chromatizing stage. The pits to be studied were searched automatically by the application of high resolution specimen digital optical scanning followed by image processing employing recognition software yielding database containing probable pits centre coordinates and its equivalent diameters

(areas to be scanned). These data were used by the SVET/conductometer scanning equipment for surface mapping.

Pits having equivalent diameter from about 5 μm as the one shown in Fig. 3 up to about 700 μm were studied. The low limit of the pit size was determined by the digital optical scanner resolution.

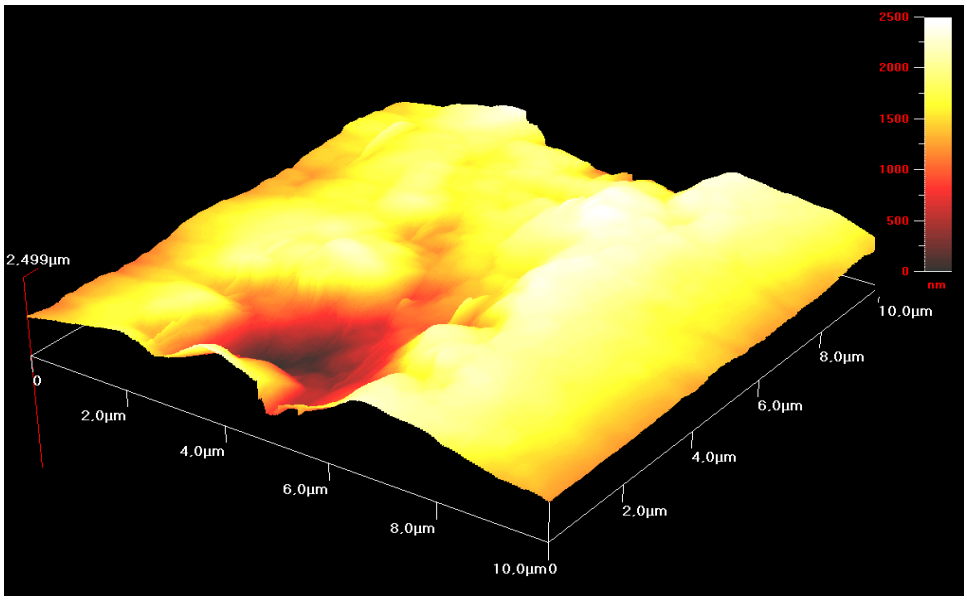

Figure 3. AFM image of the pit studied by SVET/EC

In Fig. 4 is presented a complete 3D SVET map of the current densities distribution above the pit shown in Fig. 3. The conductivity scanning performed simultaneously showed no changes in the local solution conductivity above the pit or at least these changes are smaller than the noise level. The small equivalent diameter of the studied pit may serve as one of the probable explanations of this fact. It is more probable however that the self-sealing of the porous layer and barrier layer formation occurring during the immersion in testing solution prevent the conductivity changes. Unfortunately the SVET/conductometer equipment is not sufficiently rapid to register this process occurring very rapidly since the measuring unit needs time for the positioning above the studied pit.

Although the mechanisms of chromate inhibition of the corrosion rate of Al alloys to remain still unclear the chromate-containing coatings protects mainly the damaged areas (18, 19). Several redox reactions are possible, including direct oxidation of metal substrates.(29,30) may occurs provoked by the oxidizing power of CrO_4^{2-}. In these processes the Cr^{6+} is reduced to Cr^{3+} and as a consequence, composite oxide/hydroxide adherent films are formed with the general composition xAl_2O_3/yCr_2O_3 or $xAl(OH)_3/yCr(OH)_3$, where x and y are variable, depending on conditions (20). The negative charge on CrO_4^{2-} (or $Cr_2O_7^{2-}$) facilitates migration of Cr^{6+} to anodic sites where such passivation processes occur. Based on these facts lead one may concludes that the local conductivity above the bare metal pit zones undergoes changes during its contact

with the NaCl test solution due to the metal dissolution. The presence of chromate however provokes pits sealing and hence no local solution conductivity changes occurs.

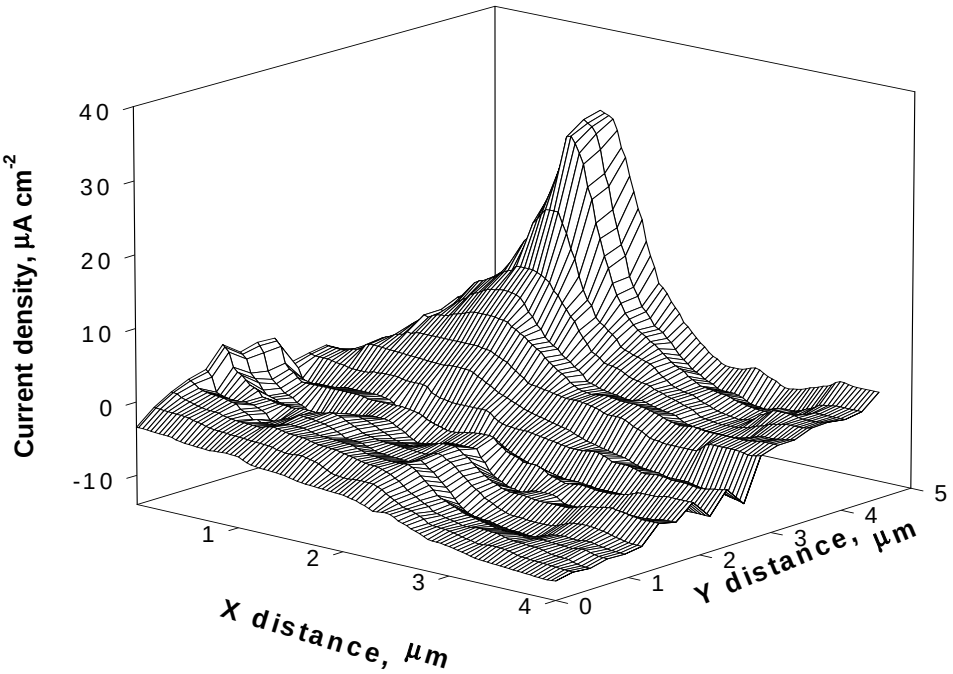

Figure 4. SVET map of the current density distribution above the pit shown in Figure 3

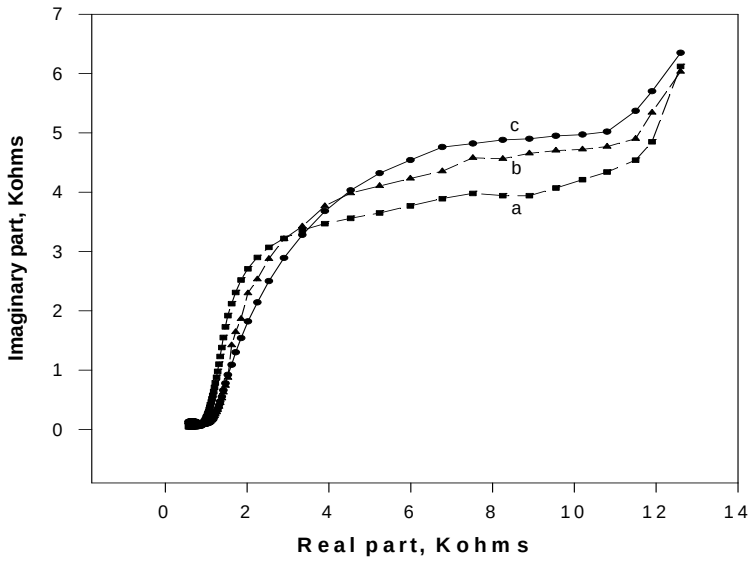

Figure 5. Nyquist curves of chromatized Al 6061-T3 aluminum alloy specimen in 5% NaCl. From surve **a** to curve **c**: 5; 10 and 20 min after the immersion

The chromatized specimen pits self sealing was confirmed by EIS experiments as well: as seen from Fig. 5 the registered Nyquist curve shows a capacitive behavior. Curve **a** corresponds to the very beginning of the corrosion process while curves **b** and **c** are related to the corrosion process in progress demonstrating an improvement of the corrosion resistance most probably due to the pits sealing.

Determination of the Software Reliability Percentage

While all the probable pits having equivalent diameters more than 15 μm were 100% recognized by the software, its reliability percentage decreased to 90.6 % together with the decrease of the pits size to 5 μm compared with the microscopic observation results. The average number of the "false" pits (pits-like stains) was found to be about 9 % of the discovered real pits. While the recognition of some false pits cause extension of the SVET measuring time only, the omitting of some real pits causes software reliability decreasing. That is why the recognition threshold of the software was chosen low and all pits having 50% or more calculated probability were included in the data base to be scanned by the SVET/conductometry equipment.

Conclusions

An approach allowing fast pits searching was applied, based on a high resolution specimen digital scanning coupled with image recognition software application yielding probable pits coordinates database used further for automatic SVET scanning of the probable pit sites only jumping over the unaffected areas.

The controversial statements of Oltra et al. (11) and Deshpande (15) about the local conductivity changes of the SVET test solution affecting the results obtained by this measuring technique were verified combining the SVET with local conductivity measurements simultaneously. It was found that no changes occurs in case of chromatized by alodining process AA 6061 - T6 specimens, while in the case of bare specimens the conductivity changes are 10 fold higher that these stated by Deshpande (15). Being about 4% only, they can not be considered as "significant", as claimed by Oltra et al. (11).

Acknowledgments

Rogelio Ramos Irigoyen acknowledges CONACyT, Mexico for the grant received to complete his Ph. D. thesis work (Programa de Maestría y Doctorado en Ciencias e Ingeniería, Instituto de Ingeniería, UABC).

References

1. L. Jaffe and R. Nuccitelli, *J. Cell. Biol*., **63,** 614 (1974).
2. H. S. Isaacs, in: *Localized Corrosion*, R. Staehle, B. Brown, J. Kruger and A. Agarwal, Editors, Vol. 3, p. 158, NACE International, Houston, (1974).
3. H. S. Isaacs, *J. Electrochem. Soc*., **138**, 722 (1991).
4. C.Wagner, *J. Electrochem. Soc.*, **98**, 116 (1951).
5. H. S. Isaacs and Y. Ishikawa, *J. Electrochem. Soc.,* **132**, 1288 (1985).

6. S. Fujimoto and T. Shibata, *Denki Kagaku*, **64,** 967 (1996).
7. R. S. Thornhill and U. R. Evans, *J. Chem. Soc*., 614 (1938).
8. R. S. Thornhill and U. R. Evans, J. Chem. Soc., 2109 (1938).
9. E. Gileadi, E. Kirowa-Eisner and J. Penciner, *Interfacial Electrochemistry: an experimental approach*, p. 216, Addison-Wesley Publishing Co., Inc., Reading, MA (1975).
10. K. R. Trethewey, D. A. Sargeant, D. J. Marsh and A. A. Tamimi, *Cor. Science*, **35,** 127 (1993).
11. R. Oltra, in: *Local probe techniques for corrosion research*, R. Oltra, V. Maurice, R. Akid and P. Marcus, Editors, European Federation of Corrosion Publications, number 45, CRC Press, Woodhead Publishing and Maney Publishing, Cambridge England, (2007).
12. K. Ogle,V. Baudu, L. Garrigues and X. Philippe, *J. Electrochem. Soc.*, **147**, 3654 (2000).
13. J. O. Park and H. Böhni, *Electrochem. Solid-State Lett*., **3**, 416 (2000).
14. B.Vuillemin, X. Philippe, R. Oltra, V. Vignal, L. Coudreuse, L. C. Dufour and E. Finot, *Corros. Sci.*, **45,** 1143 (2003).
15. K. B. Deshpande, *Corrosion Science* **52**, 2819 (2010)
16. Jie He, V. J. Gelling, D. E. Tallman and G. P. Bierwagenb, *.l Electrochem. Soc.,* **147**, 3661 (2000).
17. N. N. Voevodin, V. N. Balbyshev, M. Khobaib and M. S. Donley, *Progress in Organic Coatings*, **47**, 416 (2003).
18. H. Wienand and W. Ostertag, *Modern Paint Coat.,* **November,** 38, (1984).
19. G. Adrian and A. Bittner, *J. Coat. Technol.,* **58,** 59 (1986).
20. Z. Szklarska-Smialowska and R. W. Staehle, *J. Electrochem. Soc.,* **121,** 1146 (1974).